SECED 2023 Conference
Earthquake Engineering & Dynamics for a Sustainable Future
14-15 September 2023, Cambridge, UK

FRACTURE SIMULATION, AND EXPERIMENTAL STUDY ON STEEL DAMPER

Ferit GASHI[1], Francesco PETRINI[2] & Franco BONTEMPI[3]

***Abstract**: This paper summarizes the experimental campaign carried out for the development of a new steel energy dissipative devices named Slit Dampers (SDs) designed for earthquake protection of structures. SDs consist in shear steel plates with appropriately shaped cut-out portions of material for allowing maximum spread of plastic deformation along the device and then maximizing the hysteretic dissipative behaviour. A total of eighty-two steel shear plates with different openings and thicknesses are tested to investigate their behaviour under cyclic pseudo-static loading. Six types of steel shear plates are studied, including the SD with narrow slits that divide the plate into rectangular links, and the butterfly fuse with a diamond-shaped opening that create butterfly shape links in the plate. Other varying test parameters are loading rate, material strength, and the number of in-parallel damper elements. It is expected that the proposed model can be successfully used to predict the behaviour of dampers in real-world applications.*

Introduction

Passive control structural systems with seismic dampers have achieved significant progress in recent decades. During a major earthquake, a large amount of energy is being pumped into the building. The way in which this energy consumed in a structure determines the level of damage. If this energy can be controlled and distributed independently of structural components, seismic performance and the response of the structure will be significantly improved.
This can be achieved using the passive control system of structures. Structural control systems can be divided into three classes: passive, active, and semi-active. Passive control systems are structures equipped with devices for energy distribution that do not require an external power source for vibration response while active ore semi-active control systems are the external source of energy for the operation of actuators which supply the control forces in the structure.
This paper investigates the use of the slit and honeycomb type steel plates as the energy dissipation device for seismic application as shown in Fig.1. The hysteretic behaviour and energy dissipation capacity is evaluated via component tests under cyclic loads.
Finally, seismic performance test on large-scale structure was conducted to further verify the feasibility and effectiveness of the new seismic damper.

Research Objectives

Numerous studies have been reported on the design of steel plates with cracks or openings. Previous research has shown steel plates with slit, or openings can potentially provide a simple and cost-effective solution. three types of fuse geometries are chosen in this study to be further investigated, including plates with straight slits referred to as the slit fuses and plates with butterfly. where thin fuses are defined as having width to thickness L/t =200/20=10, 20,25, 50. In this study, seven steel damper specimens were made from mild steel plate and using cutting waterjet with specific geometry (Figure 2a, Fig.2b). The tests were performed in the Structural Laboratory of Sapienza University of Rome. The aim of the test is to determine which among

[1] Department of Structural and Geotechnical Engineering, Sapienza University of Rome, Italy
Gashi.1670547@studenti.uniroma1.it
[2] Assistant Professor, Department of Structural and Geotechnical Engineering, Sapienza University of Rome
[3] Professor, Department of Structural and Geotechnical Engineering, Sapienza University of Rome

the two proposed dampers has large energy absorption capabilities, stable hysteresis loop, and adequate stiffness.

In this study, fatigue tests were performed to clarify the low cycle fatigue characteristics of the slit and butterfly. From the experimental results, the fatigue characteristics were used with constant amplitude. In addition, a modified low-cycle fatigue relationship that incorporates the effective stiffness was proposed in order to derive more realistic fatigue characteristics that can consider the mean deformation and loading sequences. Finally, a hysterical bilinear model is introduced to represent the cyclical behaviour of the proposed system in a simple way. The validity of the forecast rigidity and strength and adaptability of the model hysteretic examined by comparing the results of the test of cyclic loading.

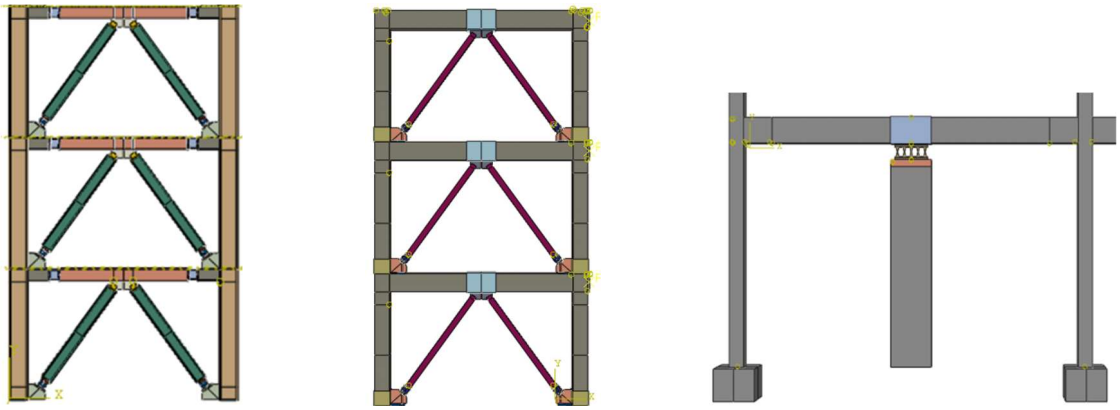

Figure 1 – Use of dampers as part of bracing and wall type systems

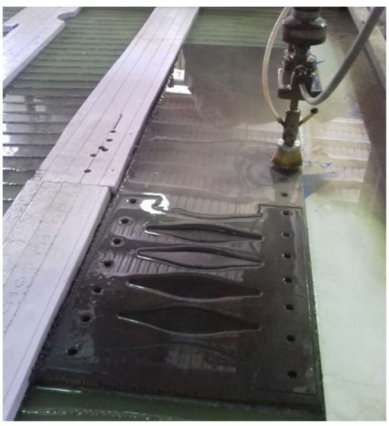

Fig.2a Shows the water cutting process

Fig.2b After water cutting.

Design of the device

Various types of cyclic tests were performed using a 500 kN hydraulic servo fatigue test machine, The MTS controller received commands from the control computer, and sent signals to the actuator, it also received back displacement and force readings for the actuator, Time history. A total of eight samples with specific geometry were cut using the water jet machine to take shape and precise dimensions. The specimens were designated as SpecimentA1, SpecimentA2, and SpecimentA3, SpecimentB1, SpecimentB2, SpecimentB3 SpecimentB4, SpecimentB5.

The eight specimens were subjected to a displacement amplitude loading pattern, AISC Modifiable. (Figure 4). The AISC protocol was modified by adding three extra sets of six low amplitude cycles and five specimens underwent constant cycles until fracture Shear deformation is defined a γ=Δ/L where Δ Horizontal displacement, h-distance HBE-330 line (360 mm).
The tests were performed until the complete failure of specimens.

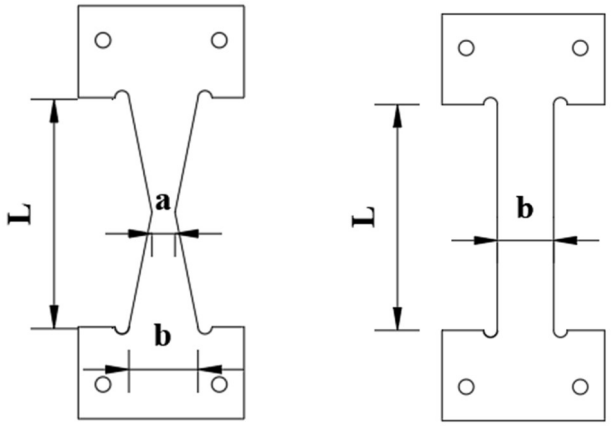

Fig.3 Geometric design of Steel Dampers

Elastic moment of bending in the slit, under sufficient displacement, plastic hinges are formed at both ends of each strip. Consequently, the mechanical properties of the crack absorber can be described in relation to the length of the strip L0, strip depth b, and thickness t(Fig.3).
Supposing elastic behaviour perfect plastic, the device gives the load P_y can be determined based on an analysis of the plastic mechanism.

Specimens	Material	Thickness	Width (mm)	Height (mm)	Loading Amp
Specimens.A1	S-235	20	60	200	Constant-A1
Specimens.A2	S-235	20	60	200	Constant-A2
Specimens.A3	S-235	20	60	200	Constant-A3
Specimens.A4	S-235	20	60	200	Constant-A4
Specimens.B1	S-235	3	60	200	Increasing-AISC
Specimens.B2	S-275	10	60	200	Increasing-AISC
Specimens.B3	S-235	20	60	200	Increasing-AISC

Table 1: Table test specimens

Experimental Program

Test Specimens

The specimen properties are listed in Table 1.

Loading Protocol

Cyclic tests were carried out on 4 specimens:
Constant cyclic loading, in which maximum displacement (Dmax) is constant over the entire cycle as 15 mm (Specimen A1), 35 mm (Specimen A2), 48 mm (Specimen A3), and 56 mm (Specimen A4). The purpose of this program is to obtain fatigue parameters.
The loading protocol for the steel damper test was created based on the AISC code loading.

The AISC protocol was modified by adding three extra sets of six low amplitude cycles preceding the prescribed loading procedure.

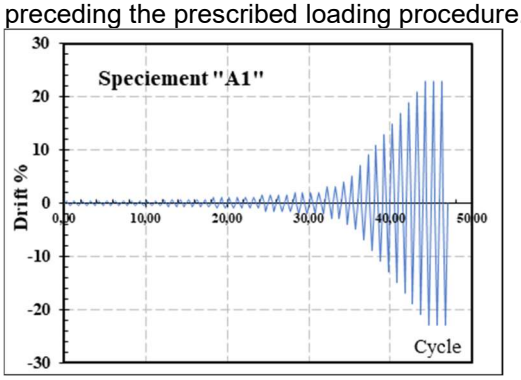

Fig.4 -AISC Modified protocol

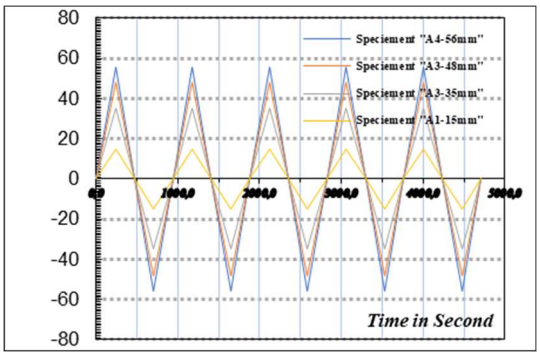

Fig.5-Constat cyclic.

Experiment Setup

Various types of cyclic tests were performed using a 500 kN hydraulic servo fatigue test machine MTS Loading was controlled by displacement with an inner displacement transducer mounted on the test machine. The loading rate (v) was fixed as 0.5 mm/s, except for incremental amplitude cycling.Fig.6

Material Properties

Plate Material Tests, five dogbone-shaped tension coupon tests were conducted on the fuse plate material. the tests took place at the Department of Structural and Geotechnical Engineering. the coupon specimens were tested using an MTS machine in fig.7

(a) (b)

Fig.7 Coupon test setup: a) Before the test, b) Necking

Set-up Metallic Dampers Testing-University of Rome La Sapienza-2020

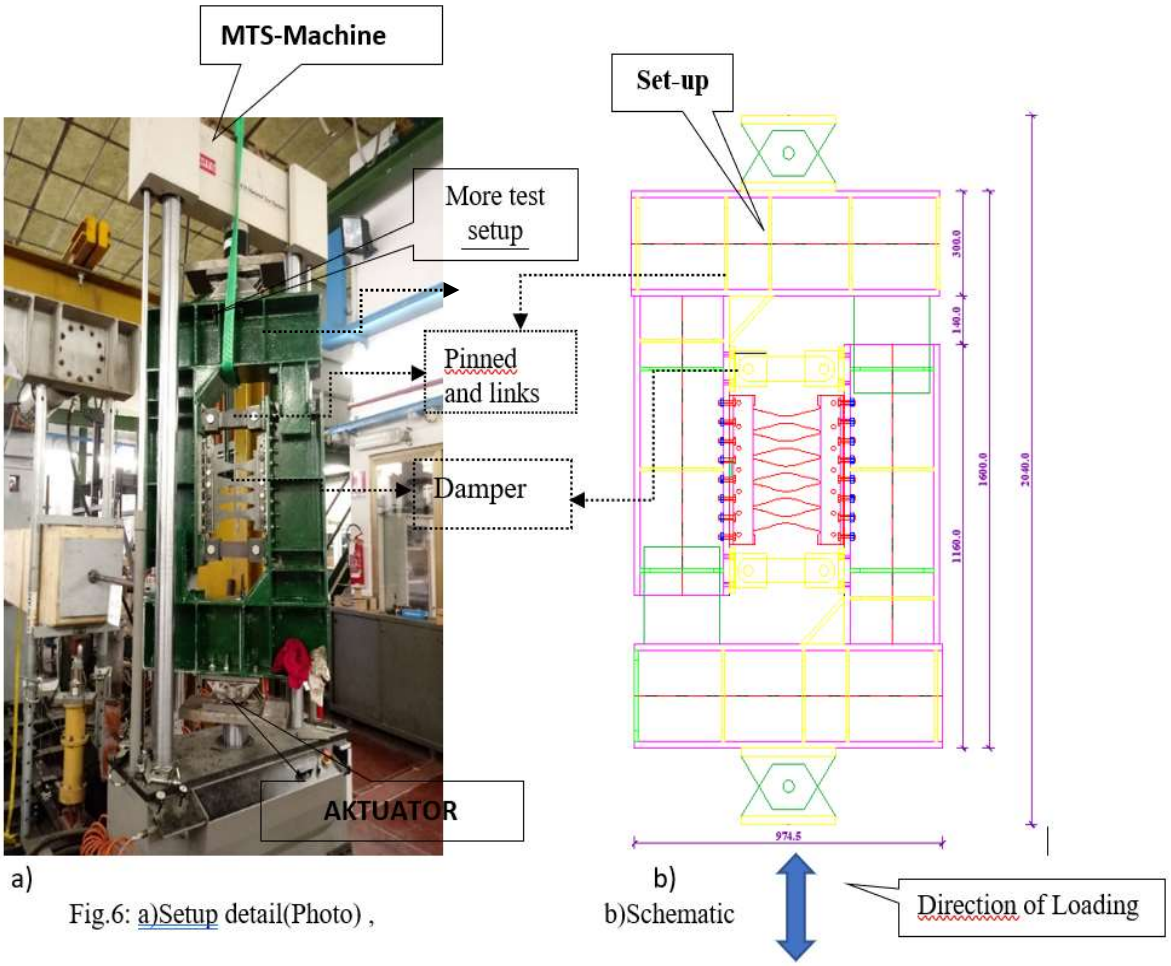

Fig.6: a)Setup detail(Photo) ,

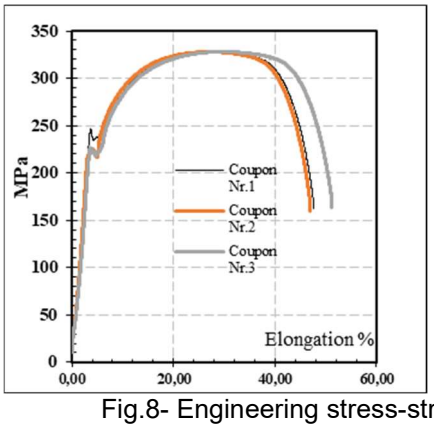

Fig.8- Engineering stress-strain curves

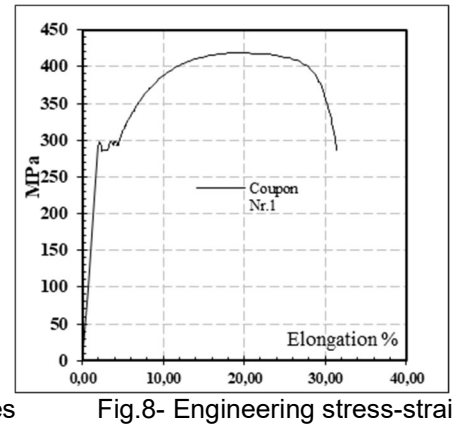

Fig.8- Engineering stress-strain curves

Three types of steel were selected: S-235, S-275. Fig.8 demonstrates their constitutive curves obtained through uniaxial tensile tests and table 2.

Coupon S-235	Fy (MPa)	Fu (MPa)	**Elongation %**	E	Coupon S-275	Fy (MPa)	Fu(MPa)	**Elongation %**	E
1	246,3	327,3	45,2	200 000	1	291,3	425,3	37,5	200 000
2	219,0	328,0	50,0	200 000	2	295,3	426,1	40,4	200 000
3	227,1	328,0	49,6	200 000					
Average	**230.8**	**327.8**	**48.3**	**200 000**	**Average**	**293.3**	**425.7**	**38.95**	**200 000**

Table 2 - Summary of mechanical properties

TEST RESULTS

Four specimens deformed stably under the cyclic tests. Specimens butterfly was loaded until fracture during the tests. Ductile cracks initiated at the toe of the butterfly close to the rounded toes of the slits during the loading of all specimens. Under further loading, those cracks propagated wider and longer, which led to the decrease of the load-carrying capacity of the dampers.

All specimens have yielded at large displacement and exhibited very stable hysteric behaviour and the shape of the loops which close to a rectangular indicates high energy dissipation capacity. Strength degradation started to appear when cracks slowly formed at the ends of the rounded corner of fixed ends due to stress concentration, which propagated longer and wider during the test until the specimen reached fracture. The tests were stopped after steel plates completely fractured, and the load sustained was significantly reduced.

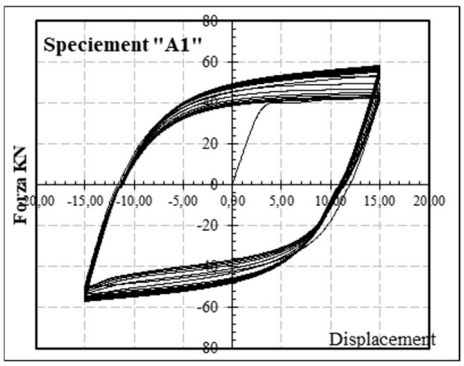

Fig.9. Force-displacement A1-15mm

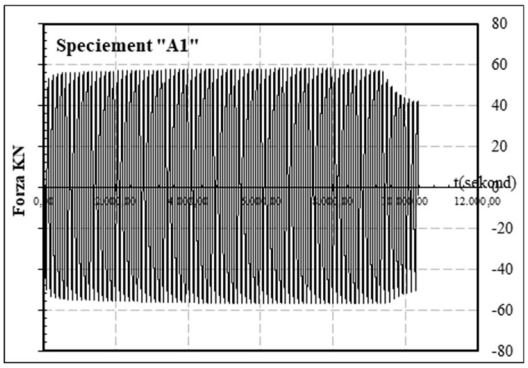

Fig.10. Time History, Force-time(s)

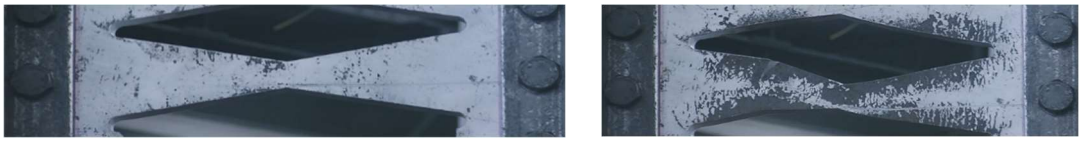

a) b)

Fig.11. Photo of Specimens A1: a Start of the test b) Fracture-end test

Link: https://www.youtube.com/watch?v=oG46PPyLIrw&t=260s

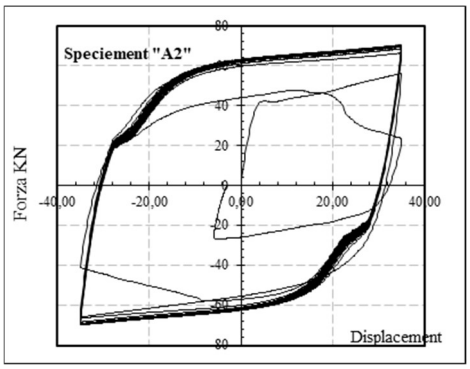

Fig.12. Force-displacement A2-35mm

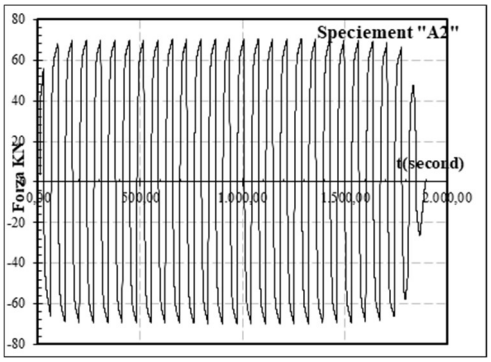

Fig.13. Time History time(s)

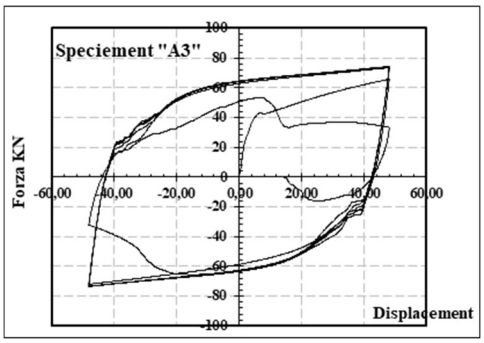

Fig.14. Force-displacement A3-48mm

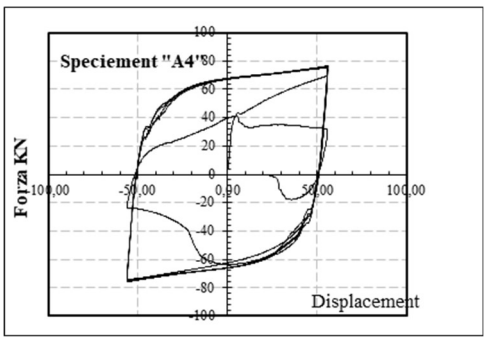

Fig.15 Force-displacement A3-56mm

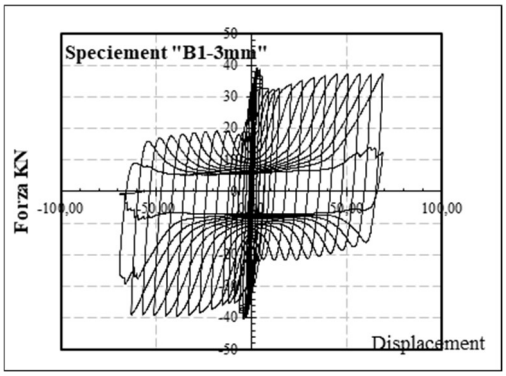

Fig.16. Force-displacement B1-3mm

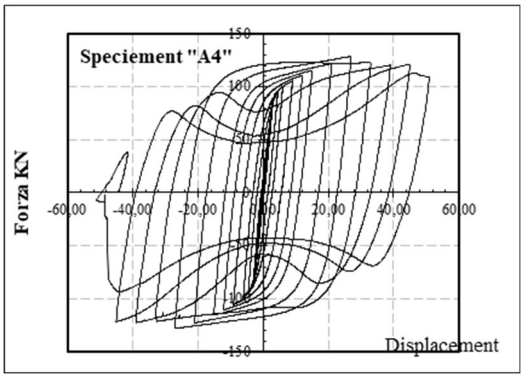

Fig.17. Force-displacement B2-8mm

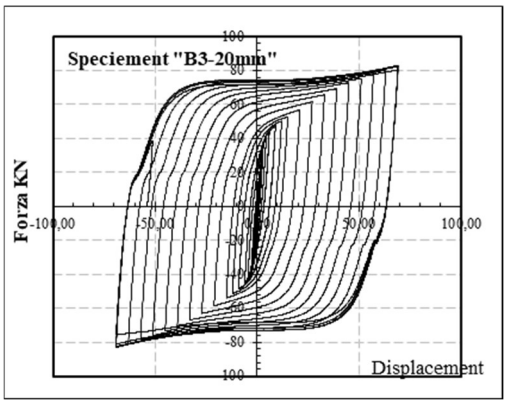

Fig.18 Force-displacement B3-20mm

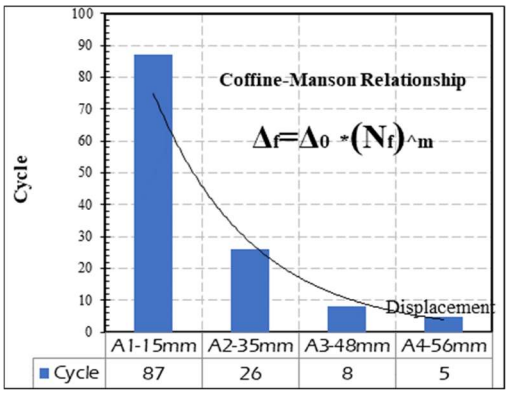

Fig.19. Low Cycle Coffine-Manson.

Energy dissipation

To investigate the effect of test parameters on the energy dissipation capacity of dampers, hysteretic curves for dissipated energy were shown in Fig.16, Fig.17, Fig.18. The dissipated energy of specimens with depth ratio (B/t) of 66.67, 25, and 10 is higher than that of specimens with depth ratio of 3mm,8mm, 20mm.

Specimens B1 with a depth 3mm, which have steel plates with the least depth variation, dissipated energy very low and failed at a relatively low cumulative displacement,Fig.16.

Specimens B2 with a depth of 8mm, which have steel plates with the least depth medium, dissipated energy very large and failed at a relatively medium cumulative displacementFig.17.

Specimens B3 with a depth of 20mm, which have steel plates with the depth large, dissipated energy very large and failed at a relatively large cumulative displacement,Fig.18.

Figure 9 shows the failure mode of the A1 specimen under constant cyclic loading. For A1, small cracks start to occur at the 78th repeated cycle. After repeatedly receiving more than 63 loads, the cracks gradually deepened at the expected plastic hinge location and finally fractured with a sudden load reduction beyond the 82nd cycle, marking the end of the experiment. The low-cycle fatigue test of the coke damper indicates that the coke damper exhibits resistance to low-cycle fatigue with sufficient inelastic deformation beyond the 82nd

cycle after yielding, and the final fracture occurs at the expected plastic locations, Fig.9.
Figure 12 shows the failure mode of the A2 specimen under constant cyclic loading. For A2, small cracks start to occur at the 24th repeated cycle. After repeatedly receiving more than 28 tensile and compressive loads, the cracks gradually deepened at the expected plastic hinge location and finally fractured with a sudden load reduction beyond the 32nd cycle, marking the end of the experiment. The low-cycle fatigue test of the coke damper indicates that the coke damper exhibits resistance to low-cycle fatigue with sufficient inelastic deformation beyond the 32nd cycle after yielding, and the final fracture occurs at the expected plastic locations.
Figure 14 shows the failure mode of the A3 specimen under constant cyclic loading. For A3, small cracks start to occur at the 6th repeated cycle. After repeatedly receiving more than 6 tensile and compressive loads, the cracks gradually deepened at the expected plastic hinge location and finally fractured with a sudden load reduction beyond the 8th cycle, marking the end of the experiment. The low-cycle fatigue test of the coke damper indicates that the coke damper exhibits resistance to low-cycle fatigue with sufficient inelastic deformation beyond the 8th cycle after yielding, and the final fracture occurs at the expected plastic locations.
Figure 15 shows the failure mode of the A4 specimen under constant cyclic loading. For A4, small cracks start to occur at the 4th repeated cycle. After repeatedly receiving more than 4 tensile and compressive loads, the cracks gradually deepened at the expected plastic hinge location and finally fractured with a sudden load reduction beyond the 5th cycle, marking the end of the experiment. The low-cycle fatigue test of the coke damper indicates that the coke damper exhibits resistance to low-cycle fatigue with sufficient inelastic deformation beyond the 5th cycle after yielding, and the final fracture occurs at the expected plastic locations.

Conclusions

The present paper presents the experimental study of steel slit-dampers with various depth. The number of loading cycles until the ultimate state of a slit-damper is found to match very well to the Manson-Coffin relation Fig.19.
The following conclusions are made from this study:
1. Damper configuration with increased height of the strip has low stiffness and provides stable hysteretic curve under large displacement irrespective of strip width at mid-height.
2. Reducing the strip width at the mid-height has a high influence on the damper performance by avoiding brittle damage at the end from stress concentration.
3. Further, varying the thickness and strip width at mid-height enhance the damping of the specimen.
4. Based on the response surface methodology, effective stiffness and effective damping is expressed as a function of strip width at mid-height (bc), height of the strip (h) and thickness of the damper (t).

Acknowledgements

The authors would like to thank prof. Dr. Franco Bontempi from the "La Sapienza" University of Rome. In addition, the authors wish to acknowledgements the technical staff at the Structural Testing Laboratory at the Sapienza University of Rome.

References

[1] Abaqus (2014). Abaqus analysis user's manual, version 16.4
[2] Aiken, I., Nims, d. Whittaker, A., and Kelly, J. (1993). "Testing of passive energy dissipation systems"
[3] Kobori, T.,Miura,Y.Fukusawa,E Yamada,T.,Arita,T..,and Takenake,Y(1992) "Development and application of hysteresis steel dampers" Proc.11th World Conference on Earthquake Engineering.
[4] Amadeo B.,Sang-Hoon OH.,Akiyama.H.(1998) "Ultimate energy absorption capacity of slit type steel plates sbjected to shear deformations
[5] ASCE. (2010). "Minimum design loads for buildings and other structures." ASCE/SEI 7-10, ASCE, Reston, VA.
[6] Dowling, N. E. (2007). Mechanical behavior of material: Engineering methods for deformation, fracture, and fatigue, 3rd Ed., Prentice Hall, NJ.
[7] Fatemi, A., and Vang, L. (1998). "Cumulative fatigue damage and life prediction theories: A survey of the state of the art for homogeneous materials." Int. J. Fatigue, 20(1), 9–34.
[8] FEMA. (2000). "Prestandard and commentary for the seismic rehabilitation of buildings." Rep. No. FEMA-356, FEMA, Washington, DC.
[9] FEMA. (2007). "Interim testing protocol for determining the seismic per-formance characteristics of structural and nonstructural components." Rep. No. FEMA-461, FEMA, Washington, DC.
[10] Ju, Y. K., Kim, M. H., Kim, J., and Kim, S. D. (2009). "Component tests of buckling-restrained braces with unconstrained length." Eng. Struct., 31(2), 507–516.
[11] Krawinkler, H., and Zohrei, M. (1983). "Cumulative damage in steel structures subjected to earthquake ground motions." Comput. Struct., 16(1–4), 531–541.
[12] Miner, M. A. (1945). "Cumulative damage in fatigue." J. Appl. Mech., 12(3), 159–164
[13] Kanvinde, A. M. & Deierlein, G. G. (2006), 'The void growth model and the stress modified critical strain model to predict ductile fracture in structural steels', Journal of Structural Engineering 132(12), 1907–1918
[14] Skinner, R. I., Kelly, J. M. & Heine, A. J. (1975), 'Hysteretic dampers for earthquake-resistant structures', Earthquake Engineering & Structural Dynamics
[15] Oh, S. H., Kim, Y.-J., and Ryu, H.-S. (2009). "Seismic performance of steel structures with slit dampers." Eng. Struct.
[16] Christopoulos C, Montgomery M. Viscoelastic coupling dampers (VCDs) for enhanced wind and seismic performance of high-rise buildings. Earthq Eng Struct Dyn 2013
[17] Chopra, A. K. (2019): Dynamic of structures. Pearson Education, 5th edition, United States.
[18] Bruneau M., Uang C.M. and Sabelli R., Ductile design of steel structures, McGraw Hill, Inc, 2011.